# Effect of carbon-negative aggregates on the strength properties of concrete for permeable pavements

Permeable pavements are engineered to temporarily store water to reduce flooding during rainfall events. Permeable pavements are distinguished primarily based on their surface materials which can vary from concrete, asphalt, clay brick, concrete pavers or plastic grids. This paper examined the effect of lightweight carbon-negative aggregates (CNA) on the behaviour of concrete intended for use as solid concrete block pavers in permeable pavements. Performance indicators targeted compressive strength, splitting tensile strength, density and water absorption. CNA were produced and sourced from manufacturing firm Carbon8 Systems in Kent U.K which applies patented accelerated carbonation technology to solidify incinerated ash into useful eco-friendly aggregates. The methodology involved substituting natural aggregates (NA) by mass, with CNA at percentages varying from 0 to 100. A scanning electron microscope was used to examine the aggregate-mortar interface. Both the compressive and tensile strengths decreased exponentially with the addition of CNA. Average 28-day compressive and splitting tensile strengths ranged from 69 MPa (10000 PSI) to 18 MPa (2600 PSI) and 3.84 MPa (560 PSI) to 1.23 MPa (178 PSI) respectively. Density values decreased linearly with the addition of CNA with average values ranging from 2200 – 2600 kg/m$^3$. Conversely, water absorption increased with increases in CNA with average values ranging from 1.66% to 9.17%. Depending on the loading requirements, CNA can replace NA in solid permeable pavement blocks by up to 100%.

Keywords: SEM, microstructure, lightweight concrete, compressive strength, permeable pavements, carbon-negative aggregate

## Introduction

Permeable pavements are engineered to perform as hybrid infrastructure. They are pavements with structural requirements typically designed to satisfy lightly trafficked surfaces such as parking lots and pedestrian access whilst promoting infiltration and stormwater runoff mitigation (Monrose and Tota-Maharaj 2018). This is significant in reducing peak flows and runoff volumes, improves stormwater runoff quality and encourages groundwater recharge where permitted. Permeable pavements supersede conventional paving with an at-source control to prevent or significantly delay stormwater runoff generation (Fassman and Blackbourn 2010).

The vertical profile of a typical permeable pavement is illustrated in Figure 1. A variety of Permeable pavements have been identified based on their surface paving material. The distinguishing factor among them is related to the total pore space, spatial arrangement of the underlying open-graded layers and structural strength. They are either monolithic, modular or grid types. Monolithic permeable pavements facilitate infiltration of water through their surfaces. Examples include porous asphalt and porous concrete. Modular pavements consist of solid permeable pavement concrete blocks placed adjacent to each other in various patterns with infiltration taking place through the joints between the blocks. The most prevalent modular units are permeable interlocking concrete pavers (PICP). Grid pavements consist of large gaps which facilitate infiltration. Examples include concrete grid pavers and plastic grid pavers (Collins 2007).

In the U.S.A., PICPs conform to ASTM C936 (ASTM 2018b) which ensures that pavers are at least 60 mm thick with a minimum compressive strength of 55 MPa. A comparative list of the minimum compressive strengths required of solid concrete block pavers (CBP) in developed nations is illustrated in Figure 2. Compressive strength requirements range from 40 MPa (New Zealand) to 60 MPa (Germany). CBP in the U.K are guided by the British Standards (BS EN 1338:2003) (BS 2003). PICPs, when designed and constructed adequately, are attractive, durable, easily repaired, require low maintenance and can withstand heavy vehicle loads (Kumar 2014). CBP can be easily replaced, thus minimising wastage of materials and construction time (Murugan et al. 2016).

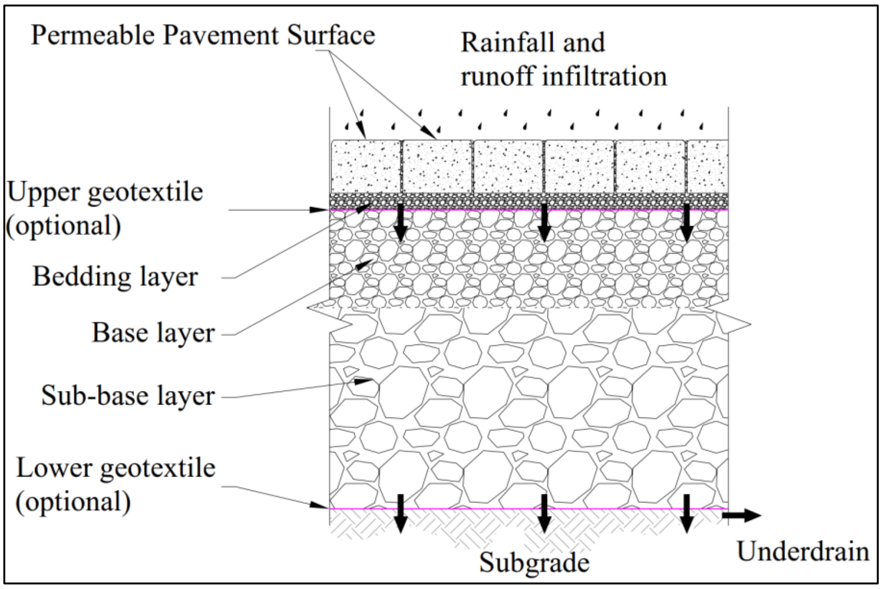


Figure 1: Vertical profile of typical permeable pavement systems with storm water runoff (source: (Monrose and Tota-Maharaj 2018))

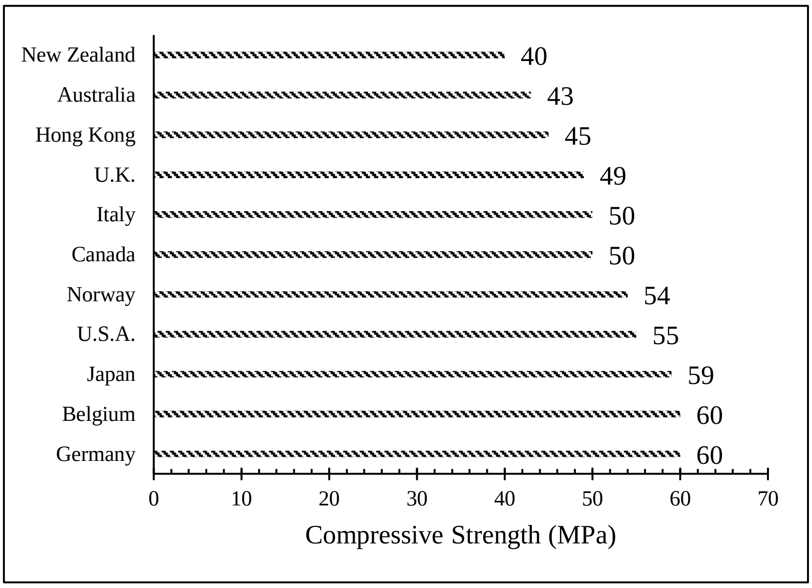


Figure 2: Minimum compressive strengths required of block pavers in various developed countries (adapted from (Jamshidi et al. 2016))

Sustainable development gears towards preserving the environment and conserving the rapidly diminishing natural resources (Rao et al. 2007). It is noticeable from Figure 1 that the typical design of permeable pavements calls for a significant quantity of quarried, virgin construction aggregates. Such large quantities may not be available in a timely manner and at the desired quantities. In the Caribbean, there is a growing demand for construction aggregates as the demand for housing and other public infrastructure increases with urbanisation. In Trinidad and Tobago for instance, the demand from the construction industry has seen a drastic increase during the past decade (Lalla and Mwasha 2014). In most recent times, however, the global economic slowdown has since resulted in a decline in construction activity. Nevertheless, the demand for civil engineering materials, construction aggregates in particular remain high (Lalla and Mwasha 2014). Innovative ways of conservation of natural aggregates are needed.

One such conservation technique is through the use of commercially-produced lightweight aggregates referred to as carbon-negative aggregates (CNA) as replacement for natural aggregates (NA) in solid concrete permeable pavement blocks. CNA were sourced from a manufacturing plant, Carbon8 Systems located in Kent, U.K. Lightweight aggregates typically possess low-particle relative densities ranging from 800 to 2000 $kg/m^3$ because of the cellular pore system (ACI 2014b). They are produced in numerous ways such as manufacturing plants from raw materials (shale, clay, slate, fly ash, slag and so on) or mined from naturally occurring volcanic deposits (pumice and scoria) (ACI 2014b).

CNA are one form of artificially engineered lightweight aggregates manufactured using Accelerated Carbonation Technology (ACT) (Fernández Bertos et al. 2004, Li et al. 2007, Gunning et al. 2010). The technology utilises carbon dioxide to pelletize municipal solid waste incinerator (MSWI) ash into potential aggregates for construction (Gunning et al. 2009).  The accelerated carbonation process captures more carbon dioxide from the waste than is used during plant processing; hence the development of a “carbon-negative” aggregate as per laboratory-based calculations. The solidified product contains permanently-bound carbon dioxide gas (Gunning et al. 2012).  The raw materials used for this production are thermal residues; for example, fly ash and Air Pollution Control residue (APCr) from waste to energy plants. The CNA are grey, sub-rounded, homogeneous, and with a rough surface (Gunning et al. 2012).

Artificially produced lightweight aggregates have been used in concrete by several academics (Al-Khaiat and Haque 1998, Haque et al. 2004, Bai et al. 2004, Kockal and Ozturan 2010, Kockal and Ozturan 2011, Terzić et al. 2015) to examine the durability, strength and stiffness of concrete. Waste materials have also been used in paving blocks by some researchers (Wattanasiriwech et al. 2009, Gencel et al. 2012, Ganjian et al. 2015, Poon and Chan 2006). Wattanasiriwech et al. (2009) investigated the use of waste mud from ceramic tile production as the main component in paving blocks. They determined compressive strengths and found that blocks containing cement ≥20 wt.% gave satisfactory strength results. Poon and Chan (2006) investigated the replacement of conventional aggregates of CBP using recycled concrete aggregate and crushed clay brick as coarse and fine aggregates respectively. The authors reported that the mechanical performance of paver blocks remain similar to that of the conventional CBP. Poon and Chan (2006) also reported that the blocks prepared using 25 wt.% crushed clay bricks as fine aggregate can achieve an adequate compressive strength for producing Grade B paving blocks in trafficked areas as prescribed by the Environment, Transport and Works Bureau Government Secretariat of Hong Kong. Gencel et al. (2012) investigated the effects of waste marble on physical and mechanical properties of CBP. The authors concluded that CBP of sufficient quality was achieved through the incorporation of marble waste.

The literature shows that a research gap exists regarding evaluations of the influence of artificial lightweight aggregates in solid CBP. This paper examines the physical and mechanical characteristics of concrete comprising CNA for use as solid CBP in permeable pavements. The methodology involves substituting NA by mass, with CNA at percentages of 0, 15, 30, 50, 75 and 100. 28-day compressive and splitting tensile strengths and water absorption tests are evaluated and compared. The mix designs ensured that cement and fines content remained unchanged irrespective of the NA/CNA ratio.

## Materials and methods

### *Materials*

Ordinary Portland Cement (OPC), CEM I 42 obtained locally in Trinidad was used in the production of all concrete mixes. OPC is manufactured in accordance with international standards (ASTM 2017c, EN 197-1 2011). Ordinary pipe borne water was used in all mixes. Quarried basalt aggregates were used as NA. CNA was supplied by manufacturing plant, Carbon8 Systems located in Kent, U.K. NA and CNA were used in the mixes as per ASTM C33 (ASTM 2016a) and ASTM C330 (ASTM 2017b) respectively. The CNA, shown in Figure 3, are porous, grey, sub-rounded, homogeneous, and rough on the surface. The chemical composition of CNA was determined by the use of an X-ray fluorescence spectrometer (XRF) and is presented in Table 1 along with the chemical composition of OPC. Natural ‘river’ sand (NS) constituted the majority of the fines component in the mixes. Conplast SP430 super plasticizer was used to improve the workability of the concrete mixes.  The physical properties of the aggregates and fines are presented in Table 2. The variations in physical and mechanical properties of the CNA and NA are very noticeable from Table 2. CNA are categorised as lightweight because of a low bulk density value below 1200 kg/m$^3$ (González-Corrochano et al. 2009). It is noteworthy that the pH of the CNA was highly alkaline; 12.26 which is in the pH range of MSWI fly ash circa 12-12.5 (Li et al. 2007). A lower pH of 7-10 was expected after carbonation as the calcium hydroxide is transformed to calcium carbonate (Li et al. 2007). The particle size distributions of the aggregates were obtained in accordance with ASTM C136 (ASTM 2014b) and are presented in Figure 4. The gradations of the CNA and the NA for concrete were obtained as per ASTM C330 (ASTM 2017a) and ASTM C 33 (ASTM 2018a) respectively.


Figure 3: Carbon-negative aggregates (CNA)

Table 1: Chemical composition of CNA and cement (% by weight)

| Oxide (wt%) | CNA | OPC (CEM I 42)[a] |
|---|---|---|
| CaO | 48.69 | 65.39 |
| $SiO_2$ | 19.65 | 22.06 |
| Cl | 14.58 | - |
| $Na_2O$ | 3.87 | 0.2 |
| C | 2.75 | - |
| $Al_2O_3$ | 2.64 | 4.25 |
| $K_2O$ | 2.34 | 0.5 |
| $Fe_2O_3$ | 1.74 | 0.02 |
| S | 0.89 | - |
| ZnO | 0.79 | - |
| $P_2O_5$ | 0.73 | - |
| MgO | 0.66 | 1.13 |
| $TiO_2$ | 0.38 | - |
| PbO | 0.13 | - |
| MnO | 0.07 | - |
| SrO | 0.04 | - |
| $Cr_2O_3$ | 0.04 | - |

| | | |
|---|---|---|
| $ZrO_2$ | 0.01 | - |

[a]Source: (Mwasha 2009)

Table 2: Physical properties of aggregates and fines

| Property | Specification | Sand | NA | CNA | Typical value |
|---|---|---|---|---|---|
| Specific Gravity, $G_s$ (kg/m$^3$) | ASTM C127 (2015) | - | 2.709 | 1.602 | |
| Water absorption (%) | ASTM C127 (2015) | - | 1.2 | 23.6 | <10 |
| LA Abrasion (%) | ASTM C131 (2014a) | - | 18 | 66 | |
| Impact (%) | BS 812 (1990b) | - | 16 | - | |
| Bulk Density (Loose) (kg/m$^3$) | ASTM C29 (2016b) | 1736 | 1530 | 1141 | |
| Fineness modulus | | 3.19 | 5.71 | 4.69 | 3.2 – 4.2 |
| Coefficient of uniformity ($c_u$) | | 4 | 2 | 8 | >4 |
| Coefficient of curvature ($c_c$) | | 1 | 1 | 1 | $1 \leq Cc \leq 3$ |
| Voids ratio | | - | 0.433 | 0.285 | |
| Porosity (%) | | - | 30 | 22.2 | |
| pH | BS 1377 (1990a) | - | 8.51 | 12.26 | 6 - 11 |

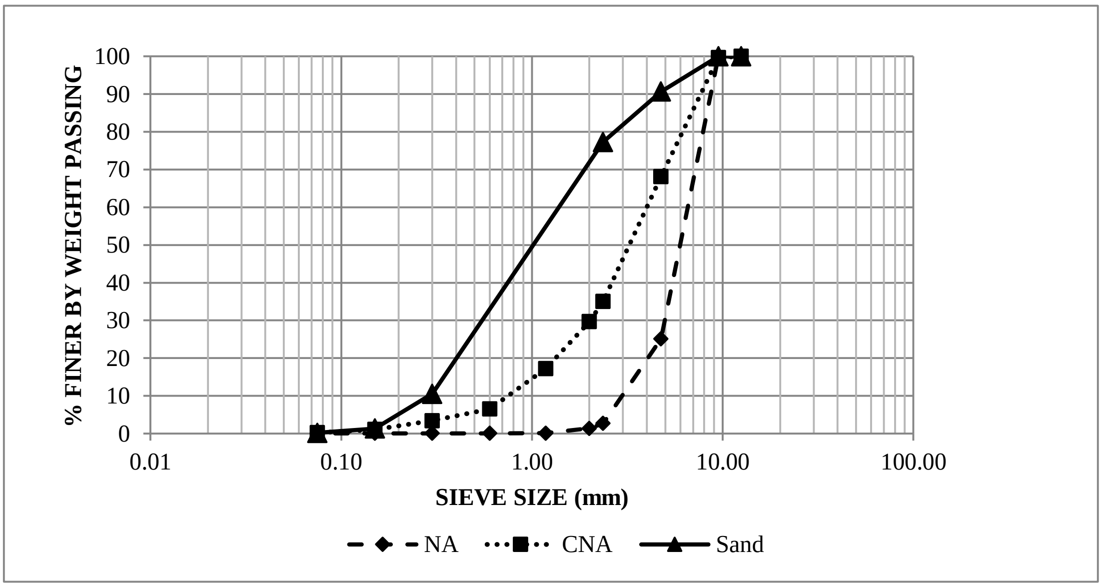


Figure 4: Particle Size Distributions (PSD) of aggregates and fines

## *Methods*

### *Production of concrete samples and solid concrete permeable pavement blocks*

Six different concrete mixes were produced whereby NA were replaced with CNA by mass in varying percentages of 0, 15, 30, 50, 75 and 100. All mixes were prepared in a 50 dm$^3$ capacity rotary mixer in the laboratory. Increased NA replacement had a negative effect on the workability of the fresh concrete because of the higher water absorption of the CNA. Consequently, the water-cement ratio was increased as the CNA percentages increased. The additional water was predetermined based on the water absorption of the CNA. Alternatively, the CNA could have been pre-soaked to saturation (Kockal and Ozturan 2011) or pre-wetted (Jiajun et al. 2006, ACI 2013) prior to mixing. For all mixes, the fresh concrete slump values were measured immediately after mixing. The mix compositions and slump values of all concrete mixes are listed in Table 3.

For each mix, four 100mm x 200mm cylinder samples, five 100mm cube samples and four 200mm x 100mm x 80mm solid CPB were prepared in accordance with BS EN 12390-3:2009 (BS 2009) and ASTM C936 (ASTM 2018b) respectively. All samples and blocks were secured, de-moulded after 24 hr, labelled and cured in water at a standard temperature of 20±1°C for 28 days before testing. A total of 54 samples and 24 CBP were prepared.

Table 3: Composition of various concrete mixtures

| Mix | CNA % | Cement (kg) | Sand (kg) | NA (kg) | CNA (kg) | Water (kg) | Super plasticizer (ml) | Slump (mm) | W/C ratio | A/C ratio |
|---|---|---|---|---|---|---|---|---|---|---|
| Control | 0 | 8 | 16 | 24 | 0 | 3.2 | 50 | 10 | 0.4 | 3 |
| CNA15 | 15 | 8 | 16 | 20.4 | 3.6 | 4.0 | 50 | 15 | 0.5 | 3 |
| CNA30 | 30 | 8 | 16 | 16.8 | 7.2 | 4.0 | 50 | 5 | 0.5 | 3 |
| CNA50 | 50 | 8 | 16 | 12 | 12 | 5.0 | 50 | 5 | 0.6 | 3 |
| CNA75 | 75 | 8 | 16 | 6 | 18 | 6.0 | 50 | 10 | 0.8 | 3 |
| CNA100 | 100 | 8 | 16 | 0 | 24 | 6.0 | 50 | 0 | 0.8 | 3 |

W/C – water/cement ratio

A/C – aggregate/cement ratio

*Testing of hardened concrete samples*

*Compressive and splitting tensile strength tests*

The 28-day compressive strength of the cube samples was measured in accordance with BS EN 12390-3:2009 (BS 2009). The splitting tensile strength tests of the cylinder samples were performed according to ASTM C 496 (ASTM 2017d).

*Density and water absorption*

Density and water absorption were determined in accordance with ASTM C642 (ASTM 2013).

*Micro-structural observations through SEM*

A scanning electron microscope (SEM) equipped with an Edax Energy Dispersive System (EDS) and Gatan Digscan imaging system shown in Figure 5, was used to examine the micro-structure and bonding or interfacial transition zone (ITZ) between the aggregates and the cementitious paste. The EDS was not used in this study. A total of two small (< 10mm in diameter) samples were taken from split concrete samples for examination. Samples from the control mix and the CNA100 mix were used. Several attempts were made prior to retrieving suitable samples without affecting the ITZ. A Denton Vacuum Desk II Sputter Coater, shown in Figure 6, was used to gold coat the samples for better electrical conductivity prior to placement in the electron microscope. The microscope was operated at medium vacuum and 10-30 kV accelerating voltage with magnifications ranging from X20 to X3000. All micrographs were digitised to 768 x 768 pixels.

Figure 5: Scanning Electron Microscope



Figure 6: Denton Vacuum Desk II Sputter Coater

## Results and discussion

### *Density and water absorption*

The relationship between %CNA replacement and average 28-day saturated surface dry (SSD) densities is presented in Figure 7. As seen from Figure 7, density values decrease with increases in %CNA. Eq.1 represents the best fit for these density results. This relationship can be attributed to the lower specific gravity of the CNA compared to that of the NA. Additionally, the spherical shape of the CNA reduced the packing density of the concrete mixtures. The NA on the other hand, were predominantly angular and fractured, thereby increasing the packing density of the mixes. The average 28-day SSD densities ranged from 2211 kg/m$^3$ (100% CNA mix) to 2591 kg/m$^3$ (0% CNA mix). Concrete with dry densities between 2000-2200 kg/m3 is considered as semi-lightweight (Abouhussien et al. 2015).

$$w_c = -3.98CNA + 2578 \quad (1)$$

where $w_c$ is average 28-day saturated surface dry density (kg/m$^3$) and CNA is the percentage of carbon-negative aggregates added by mass.

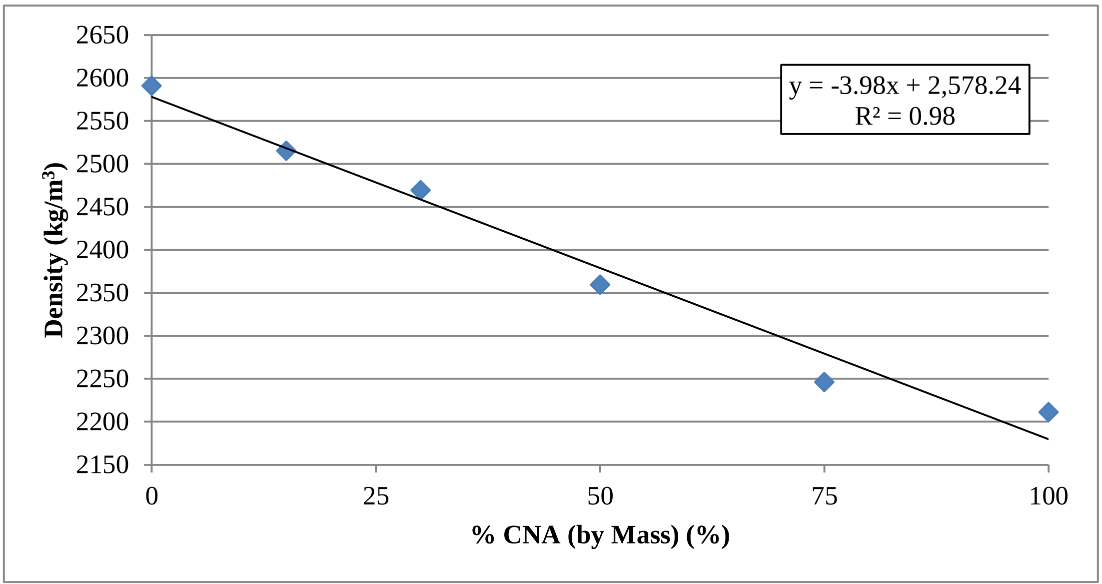


Figure 7: Relationship between average 28-day (SSD) density and percent CNA

Water absorption results are presented in Figure 8 and Figure 9. As shown in Figure 8, for all mixes, the average water absorption percentages increased rapidly during the first 20 minutes of saturation, then gradually flattened off at a slight positive gradient after 2 hours until the end of the test at 24 hours. From Figure 9, it can be seen that water absorption increased linearly with increases in CNA percent. These water absorption results can be attributed to the high porosity and high-water absorption of the CNA. The average 24-hour water absorption percentages of the various concrete mixes ranged from

1.66 (0% CNA mix) to 9.17% (100% CNA mix). Although absorption is not used as a measure of quality of concrete, most good concretes have absorption below 10% (Gencel et al. 2012).

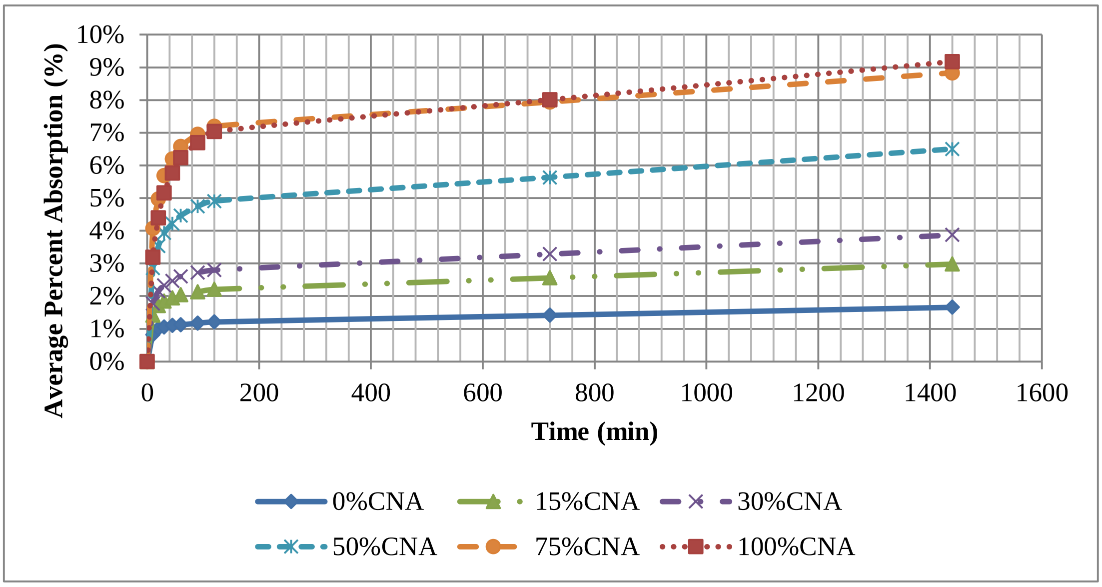


Figure 8: Water absorption rate for the various concrete mixes

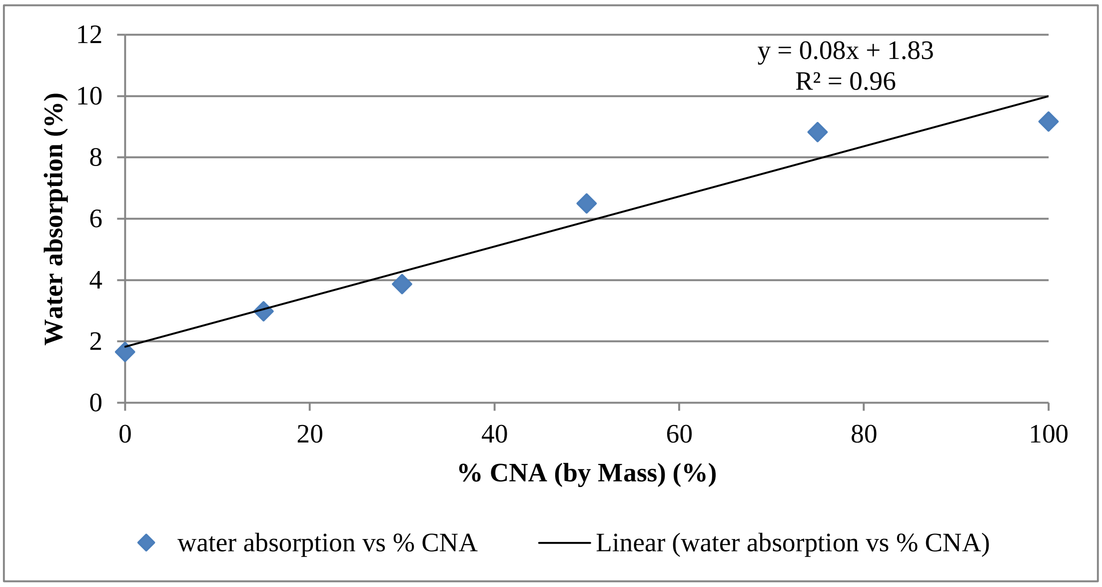


Figure 9: Relationship between water absorption and percent CNA

***Compressive Strength***

Figure 10 shows the relationship between average 28-day compressive strength values and %CNA. Compressive strengths decreased exponentially with increasing %CNA. Values ranged from 68.8 MPa (0% CNA mix) to 18.5 MPa (100% CNA mix). The reduction in compressive strength is primarily because the CNA have a significantly lower crushing resistance and density as compared to the NA. Eq. 2 represents the best fit for the results obtained.

$$f_{cu} = 66.87e^{-0.01CNA} \tag{2}$$

where $f_{cu}$ is cube compressive strength (MPa) and CNA is the percentage of carbon-negative aggregates added by mass.

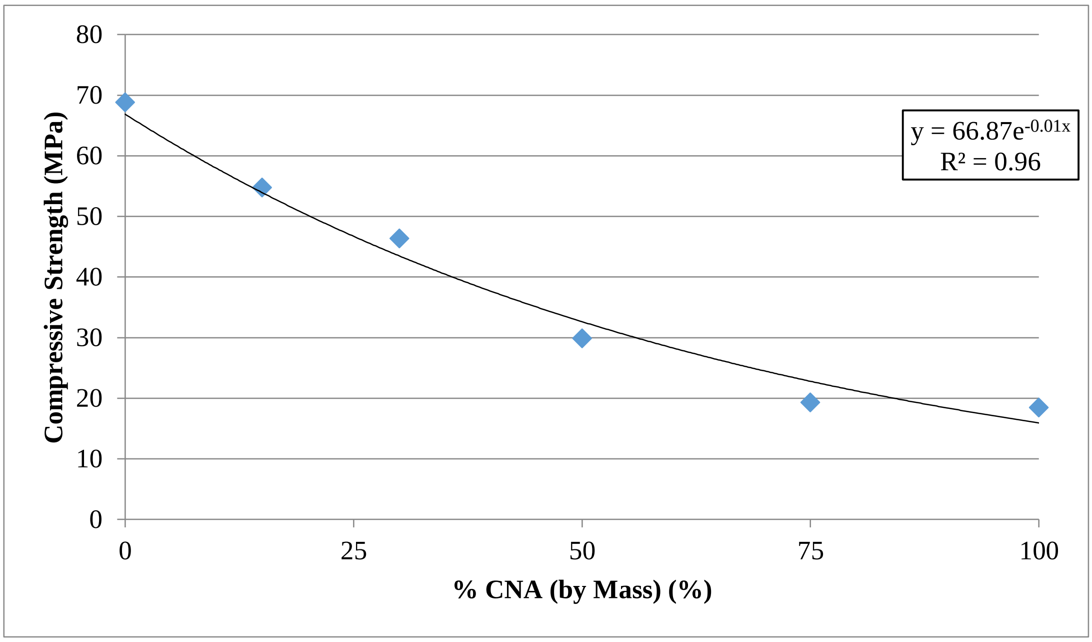


Figure 10: Relationship between 28-day compressive strength and percent CNA

Figure 11 and Figure 12 show the relationships between compressive strength and percent water absorption and between compressive strength and density respectively. For the same reasons mentioned previously, compressive strength decreased with increased water absorption and decreased density. These relationships are further presented in Equations 3 and 4.

$$f_{cu} = 89.99e^{-19.61\phi} \quad (3)$$

$$f_{cu} = 0.006e^{0.004w_c} \quad (4)$$

where $f_{cu}$ is the cube compressive strength (MPa), $\phi$ is the water absorption percentage of the CNA and $w_c$ is average 28-day saturated surface dry density (kg/m$^3$).

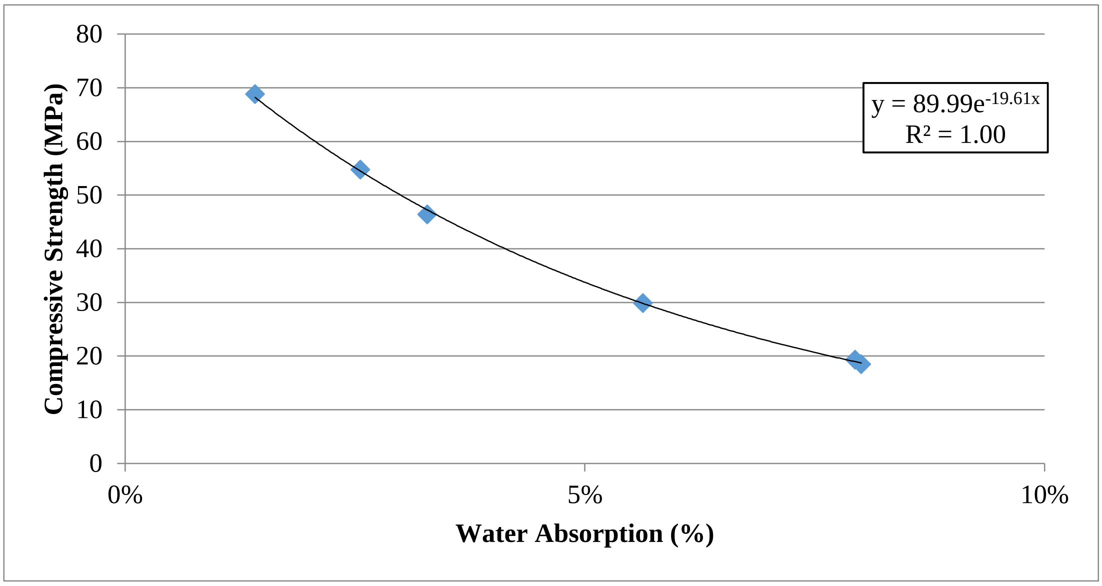


Figure 11: Relationship between 28-day compressive strength and average water absorption percent

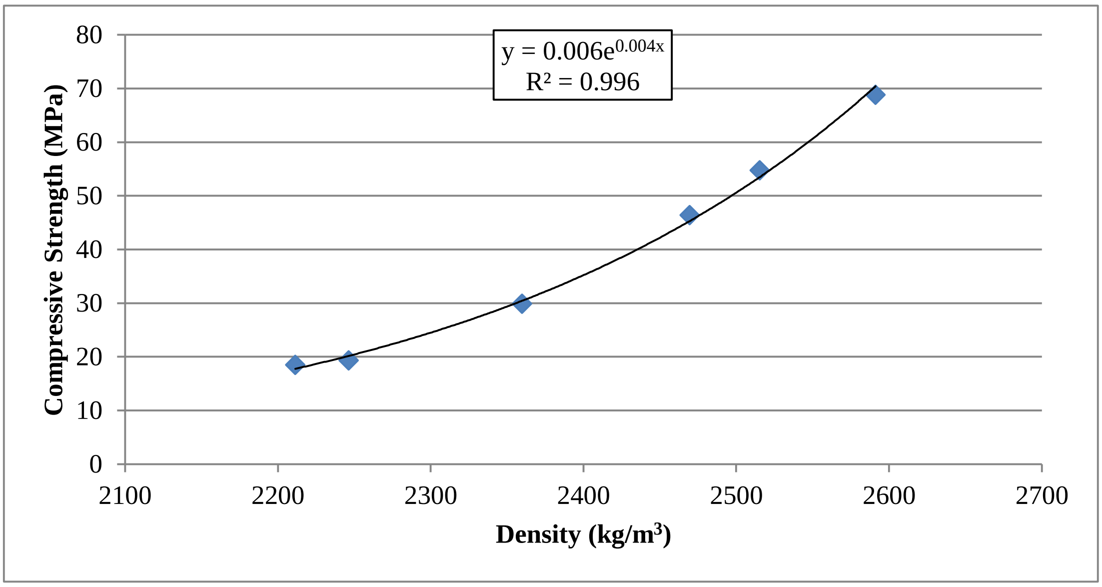

Figure 12: Relationship between 28-day compressive strength and density

***Splitting Tensile Strength***

Tensile loading is usually carried by steel reinforcement in reinforced concrete. However, it is essentially unfeasible to use steel reinforcement in solid CBP. It is necessary therefore, for a reliable assessment of the splitting tensile strength of concrete for application as solid CBP.

The average 28-day splitting tensile strength results for each mix are shown in Figure 13. As with compressive strength values, splitting tensile strengths decreased exponentially with increasing %CNA. The values ranged from 3.84 MPa (0% CNA mix) to 1.23 MPa (100% CNA mix). Again this was expected because of the physical properties of the CNA as previously discussed. Eq. 5 represents the best fit for the results. According to ASTM C330/C330M-17 (ASTM 2017b), a 28-day splitting tensile strength of 2.0 MPa is the minimum requirement for structural lightweight aggregate concrete. NA replaced with ≤50 wt.%CNA satisfied this minimum requirement.

$$f_{ct} = 3.36e^{-0.01CNA} \tag{5}$$

where $f_{ct}$ is the 28-day splitting tensile strength (MPa) and CNA is the percentage of carbon-negative aggregates added by mass.

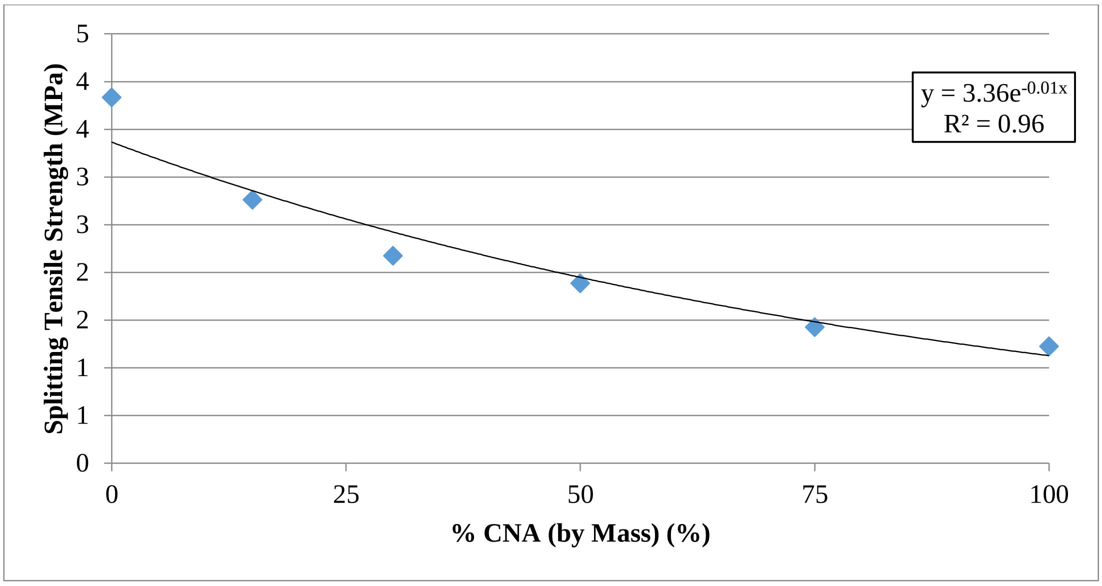


Figure 13: Relationship between 28-day splitting tensile strength and percent CNA

Images of some cylinder samples after splitting are shown in Figure 14. The predominant mode of failure of all concrete mixes was coarse aggregate failure. Minute cracks (< 2 µm) at the ITZ between the CNA and the cementitious paste were observed through SEM microstructural examination of the fractured surfaces. These cracks were insignificant, thereby confirming good bonding between aggregates and the cementitious paste.

(a) (b) (c) (d) (e) (f)

Figure 14: Photos of samples after splitting tensile strength tests (a) – 0%CNA, (b) – 15%CNA, (c) – 30%CNA, (d) – 50%CNA, (e) – 75%CNA, (f) – 100%CNA

***Relationship between splitting tensile strength and compressive strength***

Splitting tensile strength and compressive strength are widely used indices for characterising the mechanical properties of concrete (Gencel et al. 2012). Splitting tensile strength can be estimated from compressive strength using Eq. 6. An increase in compressive strength results in a general increase in splitting tensile strength.

$$f_{ct} = Af_{cu}^{B} \tag{6}$$

where $f_{ct}$ is the 28-day splitting tensile strength (MPa), $f_{cu}$ is the cube compressive strength (MPa); A and B are adjustable parameters.

Figure 15 shows the relationship between 28-day splitting tensile strength and compressive strength of the concrete mixes. Coefficient of determination ($R^2$) of the relationship was found to be 0.95 which shows satisfactory correlation. Eq. 7 represents the best fit for the results presented. For comparison, other proposed relationships (Eqs. 8 to 11) from the literature are also shown in Figure 15. Eq. 8 was proposed by Lo et al. (2016) for lightweight aggregate concrete containing sintered high-carbon fly ash aggregates with a cubical compressive strength range of 33–55 MPa. Eq. 9 was proposed by Gesoğlu et al. (2004) for lightweight aggregate concrete containing cold-bonded fly ash with a cubical compressive strength range of 20–47 MPa. Eq. 10 was proposed by ACI 318-14 (ACI 2014a) for normal weight concrete with 28-day cylinder compressive strength range of 21–83 MPa. Eq.11 was proposed by BS EN 1992 BS EN (2004).

By analysing Figure 15, it is found out that the equations provided by ACI 318, BS EN 1992, Gesoğlu et al. (2004) and Lo et al. (2016) overestimated the splitting tensile strength by on average 72%, 57%, 41% and 13% respectively.

$$f_{ct} = 0.15 f_{cu}^{0.74} \tag{7}$$

$$f_{ct} = 0.35\, f_{cu}^{0.53} \tag{8}$$

$$f_{ct} = 0.27\sqrt[3]{f_{cu}^{2}} \tag{9}$$

$$f_{ct} = 0.59\, f_{cy}^{0.5} \tag{10}$$

$$f_{ct} = 0.30\, f_{cu}^{(2/3)} \tag{11}$$

where $f_{ct}$ is the 28-day splitting tensile strength (MPa), $f_{cu}$ and $f_{cy}$ are the cube and cylindrical 28-day compressive strengths (MPa), respectively.

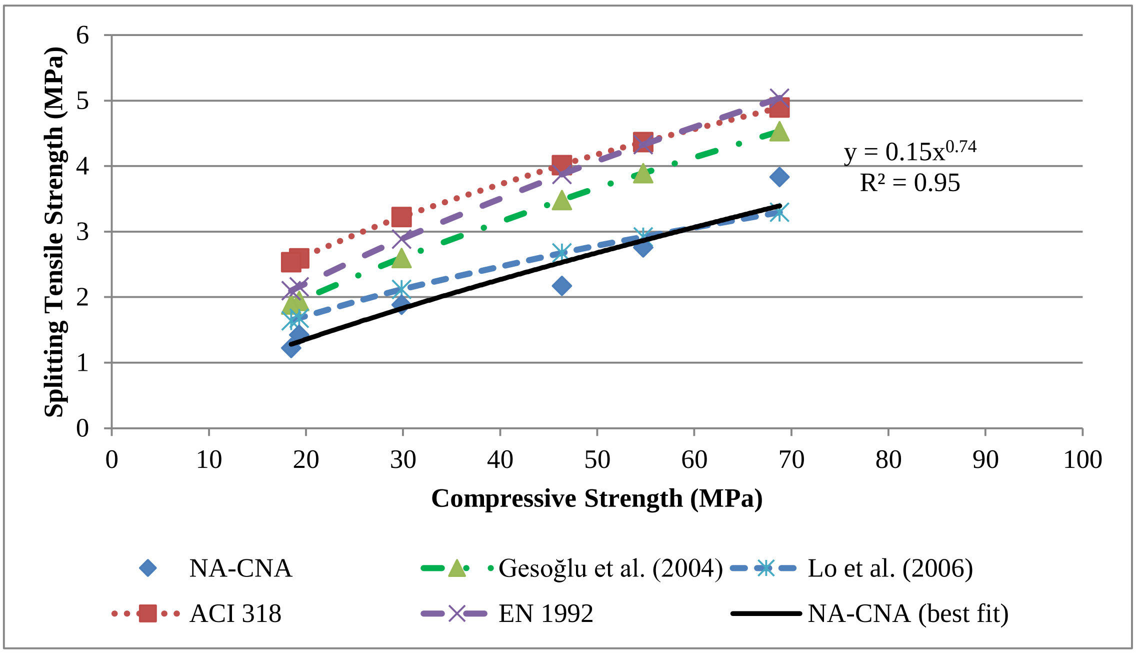


Figure 15: Relationship between compressive strength and splitting tensile strength

***SEM observations***

SEM was used to examine the micro-structure and bonding (ITZ) between the coarse aggregates (CNA and NA) and cementitious paste. Figures 16-18 show the SEM micrographs for the CNA-paste interface whilst Figure 19 and Figure 20 show the micrographs for the NA-paste interface. As mentioned previously, two samples were examined at selected points of interest along the ITZ. The cementitious paste appeared to be homogenous and dense in both samples. Overall, the bonding between the two phases in both samples appeared to be solid. The continuous hydration of the cementitious paste promotes the formation of the cementitious matrix inside the pores of the CNA therefore 'gripping' the aggregate and producing good bonding between the phases (Juan 2011). Some amount of micro-cracking (< 2 μm) was observed in both samples but appeared to be limited to the bonding zone. This separation could have occurred during the preparation of the samples for examination through SEM. This possibility was reported by Kockal and Ozturan (2010).

Further examination of the CNA revealed numerous micro-cracks (< 2 μm) in a mapped pattern over the surface of the CNA as shown in Figure 21. This was not surprising given the low strength and pozzolanic nature of the CNA.

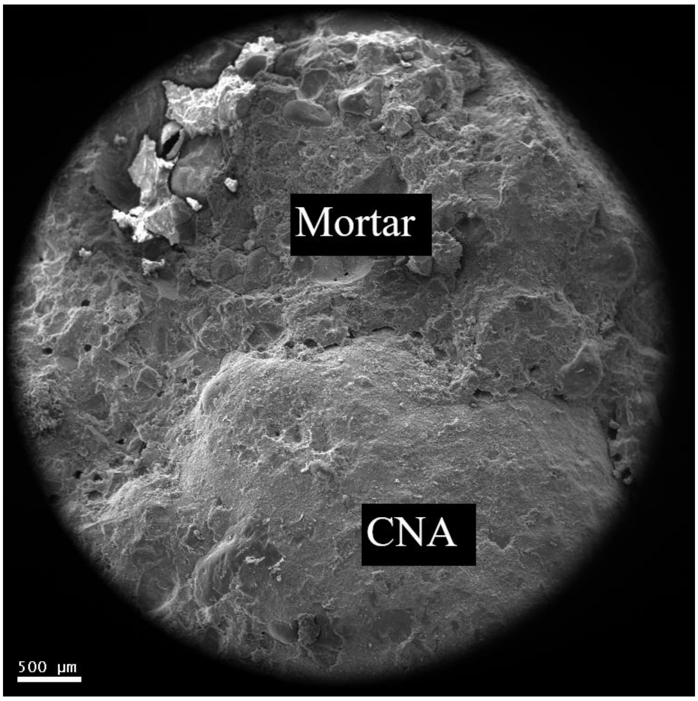


Figure 16: SEM micrograph of CNA-cementitious paste interface X 20

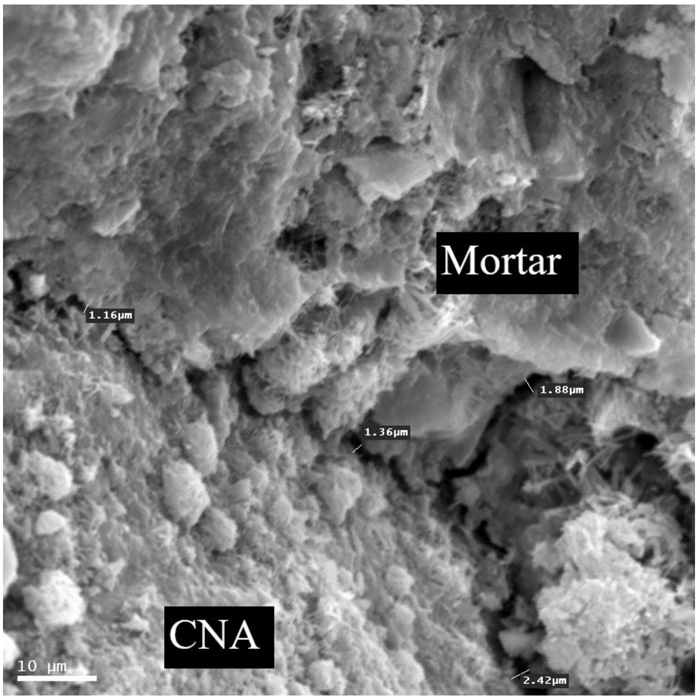


Figure 17: SEM micrograph of CNA-cementitious paste interface X 1360

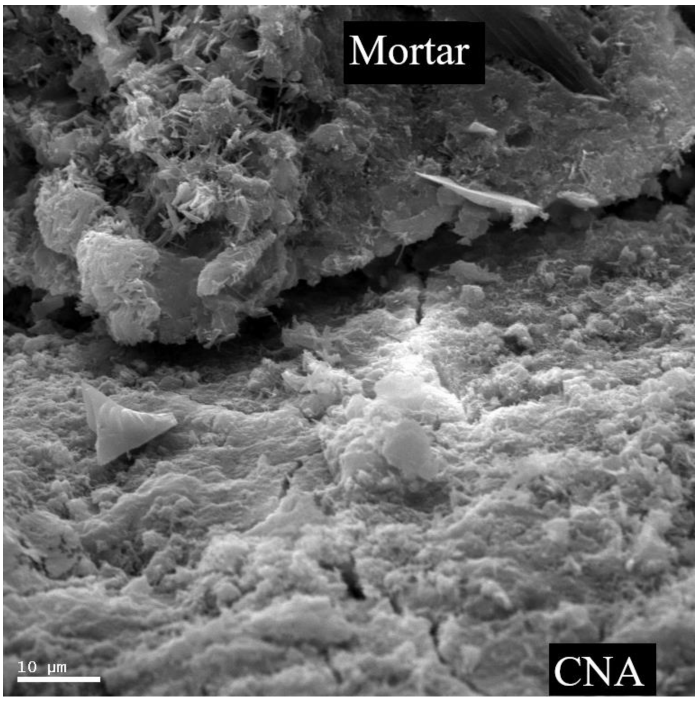


Figure 18: SEM micrograph of CNA-cementitious paste interface X 1420

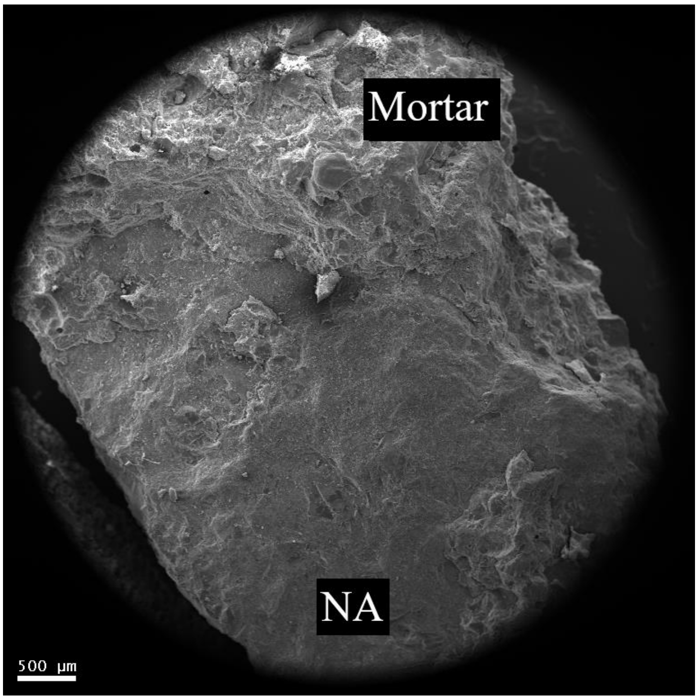


Figure 19: SEM micrograph of NA-cementitious paste interface X 20

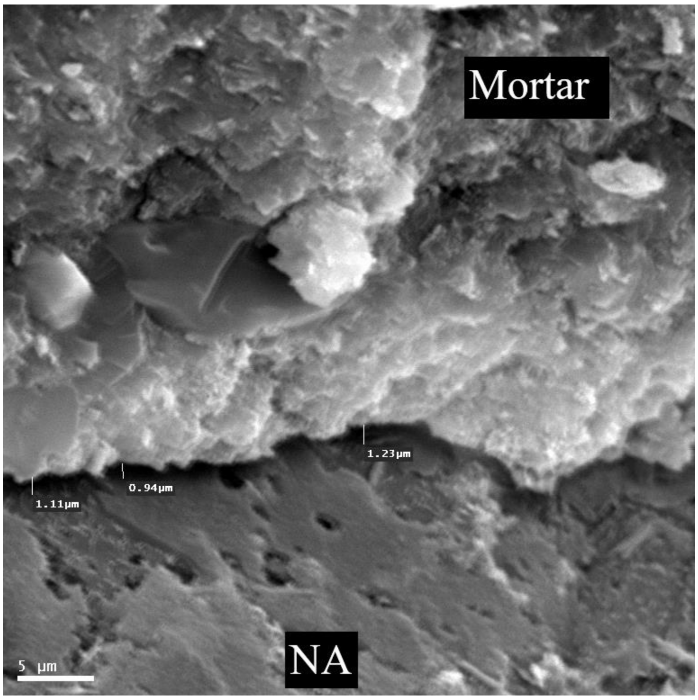


Figure 20: SEM micrograph of NA-cementitious paste interface X 2620

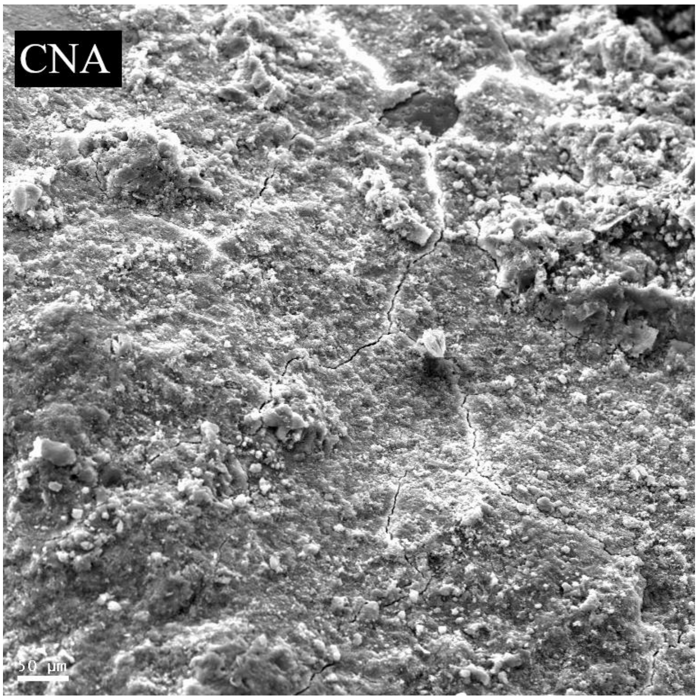


Figure 21: SEM micrograph of micro-cracking across CNA surface X 178

**Conclusion**

This study investigated the structural impact of commercially produced lightweight carbon-negative aggregates (CNA) on concrete for solid concrete block pavers (CBP) in permeable pavements. Natural aggregates (NA) were substituted by mass, with CNA at percentages of 0, 15, 30, 50, 75 and 100. 28-day compressive and splitting tensile strengths and water absorption tests were evaluated and compared. Based on the results of this study, the following conclusions are made.

(1) Depending on structural loading requirements, CNA can replace NA in solid concrete permeable pavement blocks by up to 100%.

(2) The high water absorption percent in CNA necessitates pre-soaking or increasing the water/cement ratio when increasing the mass of CNA in concrete.

(3) The 28-day compressive strengths and densities ranged from 18.48 to 68.80 MPa and from 2236 to 2612 kg/m$^3$, respectively.

(4) The 28-day splitting tensile strengths and water absorption percentages ranged from 1.23 to 3.84 MPa and from 1.66 to 9.17 %, respectively.

(5) Examination of the split aggregate-cementitious paste interfacial transition zone through SEM microstructural studies revealed good bonding results for both the CNA and NA. Further examination of the CNA revealed micro-cracks (< 2 μm) over the surface of the CNA.

(6) The use of CNA aggregates in solid concrete permeable pavement blocks is novel; presents opportunities for the conservation of rapidly-diminishing natural rocks; significantly reduces the carbon footprint during the production phase of pavements and promotes an ecologically-sustainable solution in relation to the management of municipal solid waste.

**Acknowledgements**

This research was supported by the University of the West Indies, St. Augustine Campus and international engineering firm AECOM. Special thanks to Engineer Robert Weishaupt from AECOM for his valuable input. The support of Prof Chad Staddon, Director of the International Water Securities Network (UWE, Bristol) is also acknowledged.

*The authors have declared no conflict of interest.*

**References**

Abouhussien, A. A., Hassan, A. A. A. and Ismail, M. K. 2015. Properties of semi-lightweight self-consolidating concrete containing lightweight slag aggregate. *Construction and Building Materials,* 75, 63-73.

ACI, 2013. *Report on Internally Cured Concrete Using Prewetted Absorptive Lightweight Aggregate.* MI, USA: American Concrete Institute.

ACI, 2014a. Building code requirements for structural concrete (ACI 318-14) and commentary. MI, USA: American Concrete Institute.

ACI, 2014b. Guide for Structural Lightweight-Aggregate Concrete. MI, USA: American Concrete Institute.

Al-Khaiat, H. and Haque, M. N. 1998. Effect of initial curing on early strength and physical properties of a lightweight concrete. *Cement and Concrete Research,* 28(6), 859-866.

ASTM, 2013. Standard Test Method for Density, Absorption, and Voids in Hardened Concrete. West Conshohocken, PA USA: ASTM International.

ASTM, 2014a. Standard Test Method for Resistance to Degradation of Small-Size Coarse Aggregate by Abrasion and Impact in the Los Angeles Machine. West Conshohocken, PA USA: ASTM International.

ASTM, 2014b. Standard Test Method for Sieve Analysis of Fine and Coarse Aggregates. West Conshohocken, PA USA: ASTM International.

ASTM, 2015. Standard Test Method for Relative Density (Specific Gravity) and Absorption of Coarse Aggregate. West Conshohocken, PA USA: ASTM International.

ASTM, 2016a. Standard specification for concrete aggreates. West Conshohocken, PA USA: ASTM International.

ASTM, 2016b. Standard Test Method for Bulk Density (“Unit Weight”) and Voids in Aggregate. West Conshohocken, PA USA: ASTM International.

ASTM, 2017a. Standard Specification for Lightweight Aggregates for Structural Concrete. West Conshohocken, PA USA: ASTM International.

ASTM, 2017b. Standard Specification for Lightweight Aggregates for Structural Concrete. West Conshohocken, PA USA: ASTM International.

ASTM, 2017c. Standard Specification for Portland Cement. West Conshohocken, PA USA: ASTM International.

ASTM, 2017d. Standard Test Method for Splitting Tensile Strength of Cylindrical Concrete Specimens. West Conshohocken, PA USA: ASTM International.

ASTM, 2018a. Standard Specification for Concrete Aggregates. West Conshohocken, PA USA: ASTM International.

ASTM, 2018b. Standard Specification for Solid Concrete Interlocking Paving Units. West Conshohocken, PA USA: ASTM International.

Bai, Y., Ibrahim, R. and Basheer, P. A., Properties of lightweight concrete manufactured with fly ash, furnace bottom ash, and Lytag. ed. *International Wokshop on Sustainable Development and Concrete Technology*, 2004 Beijing, 77-88.

BS, 1990a. Methods of test for soils for civil engineering purposes. Chemical and electro-chemical tests. London, U.K: British Standard Institution BSI.

BS, 1990b. Testing aggregates. Method for determination of aggregate impact value (AIV). London, U.K: British Standard Institution BSI.

BS, 2003. Concrete Paving Blocks - Requirements and Test Methods. London, U.K: British Standard Institution BSI.

BS, 2009. Testing hardened concrete. Compressive strength of test specimens. London, U.K: British Standard Institution BSI.

BS EN, 2004. Eurocode 2: Design of concrete structures Part 1-1–General rules and rules for buildings (including NA). *London: British Standards Institution.*

Collins, K. A., 2007. *A field evaluation of four types of permeable pavement with respect to water quality improvement and flood control.* MSc. Thesis. North Carolina State University.

EN 197-1, 2011. Cement - Part 1: Composition, specifications and conformity criteria for common cements. Brussels, Belgium: CEN.

Fassman, E. A. and Blackbourn, S. 2010. Urban Runoff Mitigation by a Permeable Pavement System over Impermeable Soils. *Journal of Hydrologic Engineering,* 15(6), 475-485.

Fernández Bertos, M., *et al.* 2004. A review of accelerated carbonation technology in the treatment of cement-based materials and sequestration of CO2. *Journal of Hazardous Materials*, 112(3), 193-205.

Ganjian, E., Jalull, G. and Sadeghi-Pouya, H. 2015. Using waste materials and by-products to produce concrete paving blocks. *Construction and Building Materials,* 77, 270-275.

Gencel, O.*, et al.* 2012. Properties of concrete paving blocks made with waste marble. *Journal of Cleaner Production,* 21(1), 62-70.

Gesoğlu, M., Özturan, T. and Güneyisi, E. 2004. Shrinkage cracking of lightweight concrete made with cold-bonded fly ash aggregates. *Cement and Concrete Research*, 34(7), 1121-1130.

González-Corrochano, B., Alonso-Azcárate, J. and Rodas, M. 2009. Characterization of lightweight aggregates manufactured from washing aggregate sludge and fly ash. *Resources, Conservation and Recycling,* 53(10), 571-581.

Gunning, P. J., Hills, C. D. and Carey, P. J. 2009. Production of lightweight aggregate from industrial waste and carbon dioxide. *Waste Management,* 29(10), 2722-2728.

Gunning, P. J., Hills, C. D. and Carey, P. J. 2010. Accelerated carbonation treatment of industrial wastes. *Waste Management*, 30(6), 1081-1090.

Gunning, P. J., *et al.*, 2012. Carbonation of MSWI APCr for re-use as a light-weight aggregate. *Ash Utilisation 2012 - Ashes in a Sustainable Society.* Stockholm, Sweden.

Haque, M. N., Al-Khaiat, H. and Kayali, O. 2004. Strength and durability of lightweight concrete. *Cement and Concrete Composites,* 26(4), 307-314.

Jamshidi, A.*, et al.* 2016. Performance of pavements incorporating waste glass: The current state of the art. *Renewable and Sustainable Energy Reviews,* 64(Supplement C), 211-236.

Jiajun, Y.*, et al.* 2006. Effect of pre-wetted light-weight aggregate on internal relative humidity and autogenous shrinkage of concrete. *Journal of Wuhan University of Technology-Mater. Sci. Ed.,* 21(1), 134-137.

Juan, K. Y., 2011. *Cracking Mode and Shear Strength of Lightweight Concrete Beams.* Ph.D Thesis. National University of Singapore.

Kockal, N. U. and Ozturan, T. 2010. Effects of lightweight fly ash aggregate properties on the behavior of lightweight concretes. *Journal of Hazardous Materials,* 179(1), 954-965.

Kockal, N. U. and Ozturan, T. 2011. Durability of lightweight concretes with lightweight fly ash aggregates. *Construction and Building Materials,* 25(3), 1430-1438.

Kumar, K., 2014. Review on Permeable Pavement Systems. *11th Transportation planning and methodologies for developing countries* Bombay.

Lalla, J. R. F. and Mwasha, A. 2014. Investigating the Compressive Strengths of Guanapo Recycled Aggregate Concrete as Compared to that of its Waste Material. *West Indian Journal of Engineering,* 36(2), 1.

Li, X.*, et al.* 2007. Accelerated carbonation of municipal solid waste incineration fly ashes. *Waste Management,* 27(9), 1200-1206.

Lo, T. Y.*, et al.* 2016. Manufacturing of sintered lightweight aggregate using high-carbon fly ash and its effect on the mechanical properties and microstructure of concrete. *Journal of Cleaner Production,* 112, 753-762.

Monrose, J. and Tota-Maharaj, K. 2018. Technological Review of Permeable Pavement Systems for Applications in Small Island Developing States. *CLEAN – Soil, Air, Water,* 46(9), 16.

Murugan, R. B., Natarajan, C. and Chen, S.-E. 2016. Material development for a sustainable precast concrete block pavement. *Journal of Traffic and Transportation Engineering (English Edition),* 3(5), 483-491.

Mwasha, A. 2009. Natural and Recycled Guanapo Quarzite Aggregates for Ready Mix Concrete. *The Journal of the Association of Professional Engineers of Trinidad and Tobago*, 38(1), 50-56.

Poon, C. S. and Chan, D. 2006. Paving blocks made with recycled concrete aggregate and crushed clay brick. *Construction and Building Materials*, 20(8), 569-577.

Rao, A., Jha, K. N. and Misra, S. 2007. Use of aggregates from recycled construction and demolition waste in concrete. *Resources, Conservation and Recycling,* 50(1), 71-81.

Terzić, A., *et al.* 2015. Artificial fly ash based aggregates properties influence on lightweight concrete performances. *Ceramics International*, 41(2, Part B), 2714-2726.

Wattanasiriwech, D., Saiton, A. and Wattanasiriwech, S. 2009. Paving blocks from ceramic tile production waste. *Journal of Cleaner Production,* 17(18), 1663-1668.